Mobility Studies on Sol−Gel Processed Ether−Phosphines and Their Ruthenium(II) Complexes with Different Spacer Lengths. A Solid-State NMR Study[1,2]

Ekkehard Lindner,* Andreas Jäger, Theodor Schneller, and Hermann A. Mayer[†]

Institut für Anorganische Chemie der Universität,
Auf der Morgenstelle 18, D-72076 Tübingen, Germany

Received February 28, 1996. Revised Manuscript Received August 26, 1996[⊗]

The monomeric ether−phosphine ligands $(MeO)_3Si(CH_2)_x(Ph)PCH_2CH_2OMe$ {x = number of methylene groups; x = 3 [**1a(T^0)**], 6 [**1b(T^0)**], 8 [**1c(T^0)**]} and their P-coordinated trimethoxysilyl-(T)-functionalized ruthenium complexes *cis*-$Cl(H)Ru(CO)(P{\sim}O)_3$ [**2a(T^0)$_3$**], [**2b(T^0)$_3$**], and [**2c(T^0)$_3$**] were sol−gel processed with fixed amounts of $Si(OEt)_4$ (**Q^0**), $MeSi(OMe)_3$ (**T^0**), and $Me_2Si(OEt)_2$ (**D^0**) to give the polysiloxane-bound ether−phosphine ligands [**1(a,b,c)(T^n)(Q^k,T^m,D^i)$_y$**] and the ruthenium complexes [**2(a,b,c)(T^n)$_3$(Q^k,T^m,D^i)$_y$**] [P∼O: η^1-P-coordinated ether−phosphine ligand; y = number of co-condensed Q, T, or D type; Q = Q type silicon atom (four oxygen neighbors), T = T type silicon atom (three oxygen neighbors), D = D type silicon atom (two oxygen neighbors); i, k, n, m = number of Si−O−Si bonds; i = 0−2; n, m = 0−3; k = 0−4]. Solid-state ^{29}Si NMR spectroscopy has been used to show that the matrixes containing ligands or complexes have comparable structures, independently from the employed spacer (*n*-propyl, *n*-hexyl, or *n*-octyl). Detailed ^{31}P NMR relaxation time studies (T_{1P}, T_{PH}, $T_{1\rho H}$), 2D WISE NMR spectroscopy, and the line widths of the ^{31}P CP/MAS NMR spectra have been applied for dynamic investigations. The noncomplexed ether−phosphine ligands are highly mobile and their flexibility is enhanced by longer spacers for all types of matrixes. The mobility of the ligands is also dependent upon the employed co-condensate. Functionalized F-T/Q copolymers are less flexible than F-T/T or even F-T/D copolymers [F = $-(CH_2)_xP(Ph)CH_2CH_2OMe$]. The P-coordination of the ether−phosphines in the complexes led to an additional cross-linking in the matrixes. Thereby the ligands become more rigid due to strong phosphorus−ruthenium bonds. The differences of the mobilities of the different polymer-bound complexes are smaller compared to the noncomplexed ligands.

Introduction

The preparation and application of polymer-supported transition-metal complexes, acting as catalysts, is a field of growing interest.[3,4] These systems can, in principle, combine the advantages of homogeneous with those of heterogeneous catalysis, especially if the presence of an adequate solvent or substrate (mobile phase) leads to a swelling of the polymers (stationary phase). The resulting penetration of the mobile and stationary phases on a molecular scale is called “interphase”, since no homogeneous mixture is formed. Such interphases are able to imitate homogeneous reaction conditions.[5,6] However, the activities and selectivities obtained by the various types of immobilized transition-metal catalysts are still not satisfactory and therefore technically not applicable yet. The reasons are the reduced mobilities of the active centers due to their immobilization. It is expected that the dynamic properties of the stationary phases will strongly influence the catalytic activity of the immobilized complex, e.g., that more mobile catalysts lead to more solution-like behavior and thus to higher turnover numbers and selectivities.

Inorganic oxides as carrier matrixes, e.g., synthetic silicates, have gained outstanding importance due to their diversity in physical properties, their purity and chemical resistance, their ease of functionalization through silanol groups, and their abilities to form interphases by swelling in adequate solvents.[7] In contrast to surface-modified inorganic materials,[8−10] simultaneous co-condensation of organo-T-silyl-functionalized transition-metal complexes with D, T, and Q alkoxysilanes [**Q^0** = $Si(OEt)_4$, **T^0** = $MeSi(OMe)_3$, **D^0** = $Me_2Si(OEt)_2$] (sol−gel process[11]) affords a possibility to modify these materials (see Scheme 1).[6,12,13]

---

* To whom correspondence should be sent.

[†] E-mail: hermann.mayer@uni-tuebingen.de.

[⊗] Abstract published in *Advance ACS Abstracts,* October 1, 1996.

(1) Dedicated to Professor J. Strähle on the occasion of his 60th birthday.

(2) Supported Organometallic Complexes. 11. Part 10: Lindner, E.; Jäger, A.; Kemmler, M.; Auer, F.; Wegner, P.; Mayer, H. A.; Benez, A.; Plies, E. *Inorg. Chem.*, submitted for publication.

(3) Hartley, F. R. *Supported Metal Complexes*; D. Reidel Publishing Co.: Boston, MA, 1985.

(4) Deschler, U.; Kleinschmit, P.; Panster, P. *Angew. Chem., Int. Ed. Engl.* **1986**, *25*, 236.

(5) Lindner, E.; Kemmler, M.; Schneller, T.; Mayer, H. A. *Inorg. Chem.* **1995**, *34*, 5489.

(6) Lindner, E.; Kemmler, M.; Mayer, H. A.; Wegner, P. *J. Am. Chem. Soc.* **1994**, *116*, 348.

(7) Eckert, H. *Prog. Nucl. Magn. Reson. Spectrosc.* **1992**, *24*, 159.

(8) Sindorf, D. W.; Maciel, G. E. *J. Am. Chem. Soc.* **1983**, *105*, 3767.

(9) Bayer, E.; Albert, K.; Reiners, J.; Nieder, M.; Müller, D. *J. Chromatogr.* **1983**, *264*, 197.

(10) Blümel, J. *Inorg. Chem.* **1994**, *33*, 5050.

(11) Brinker, C. J.; Scherer, G. W. *Sol Gel Science*; Academic Press: London, 1990.

© 1997 American Chemical Society

Scheme 1

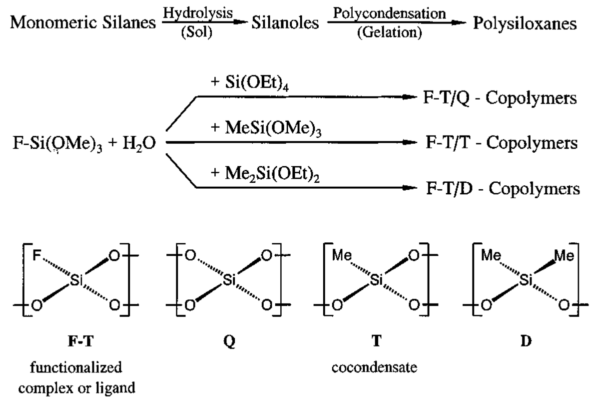

F = (Ph)P(CH_2CH_2OMe)(CH_2)$_x$- (**1a**, **1b**, **1c**)

F = [*cis*-Cl(H)Ru(CO)]$_{1/3}$P(Ph)(CH_2CH_2OMe)(CH_2)$_x$- (**2a**, **2b**, **2c**)

x = length of the spacer [x = 3 (**a**), 6 (**b**), 8 (**c**)]

Q: Q type silicon atom (four oxygen neigbors)

T: T type silicon atom (three oxygen neighbors)

D: D type silicon atom (two oxygen neighbors)

These novel materials, which we denote as stationary phases, consist of the matrix, the spacer, and the reactive center. They allow higher loading of catalysts than surface-modified silica gel in combination with reduced leaching of the reactive centers due to their high degree of condensation.[6,13] Recently it was demonstrated by stoichiometric reactions that all the reactive centers are easily accessible for substrates and that even sensitive complexes can be immobilized by the sol−gel route, using a special "trapping" technique.[14] In this new approach the reactive site of the complex is protected by a versatile ligand during the polycondensation and the catalytic active complex is subsequently generated within the matrix.

Heteronuclear cross-polarization magic-angle spinning (CP/MAS) solid-state NMR spectroscopy has been shown to be a powerful tool for investigating insoluble and noncrystalline solids.[15−17] The stereochemistry of the metal complexes, the integrity of the spacers, and the ligand backbone are established by ^{31}P and ^{13}C CP/MAS NMR spectroscopy, respectively. The structure of the polysiloxane matrixes is characterized by silicon-29 solid-state NMR spectroscopic studies. Furthermore, the dynamic behavior of the different polysiloxane-bound ether−phosphine ligands and their ruthenium complexes is described by the parameters T_{PH}, T_{1P}, $T_{1\rho H}$, and their line widths. With these data it is possible to compare the mobilities of the reactive centers on different time scales. However these methods do not allow one to gain information on the kind of motions. In addition the two-dimensional wide-line spectroscopy (WISE, vide infra) is applied to characterize the segmental mobilities of these materials.[18]

In previous studies[6,13] we were able to demonstrate that the structures and mobilities of polysiloxane matrixes strongly depend on the employed co-condensate. F-T/D type copolymers lead to a higher mobility than F-T/T or F-T/Q blends (for the meaning of F, D, T, and Q see Scheme 1) if polymer-bound ligands are considered, whereas in the case of immobilized ruthenium and palladium complexes no differences were observed {F = −(Ph)P(CH_2CH_2OMe)(CH_2)$_x$− or [*cis*-Cl(H)Ru(CO)]$_{1/3}$P(Ph)(CH_2CH_2OMe)(CH_2)$_x$−}. The P-coordination of the ligand to the metal makes the active centers uniformly rigid. In all these earlier works only ether−phosphine ligands with *n*-propyl spacers have been used.[2,5,6,13,14,19−21] In continuation of these investigations, we set out to examine if longer spacers enhance the mobilities of the reactive centers in F-T/Q, F-F/T, and F-T/D copolymers. We therefore immobilized the ether−phosphine ligands with *n*-hexyl spacers [**1b-(T^0)**][19,22] and *n*-octyl spacers [**1c(T^0)**] and compared them with the previously described species **1a(T^0)**[19] containing *n*-propyl spacers. The corresponding polysiloxane-bound ruthenium complexes *cis*-Cl(H)Ru(CO)-(P~O)$_3$, **2(a,b,c)(T^0)$_3$** [P~O: η^1-P-coordinated ether−phosphine ligand **1(a,b,c)(T^0)**] are compared as well.

Results and Discussion

Monomeric Ligands [1(a,b,c)(T^0)]^{22} and Complexes [2(a,b,c)(T^0)$_3$].^{22} The ether−phosphine ligands **1a(T^0)** and **1b(T^0)** with *n*-propyl and *n*-hexyl spacers, respectively (see Scheme 2) can be prepared in a few steps and good yields by procedures given in the literature.[19] Ligand **1c(T^0)** with a *n*-octyl spacer was synthesized by an analogous route as compound **1b(T^0)** (see Experimental Section). These "hemilabile" ligands are able to coordinate strongly to the metal center via the phosphorus atom, while the weaker donor in the form of an ether moiety is able to take over the function of an intramolecular solvent in a catalytic cycle.[23] The monomeric complexes *cis*-Cl(H)Ru(CO)(P~O)$_3$ [**3a(T^0)$_3$**, **3b(T^0)$_3$**, **3c(T^0)$_3$**; see Scheme 2] were prepared by substitution of triphenylphosphine in *cis*-Cl(H)Ru(CO)-(PPh_3)$_3$ with the more basic ether−phosphines [**1(a,b,c)-(T^0)**; see ref 6 and Experimental Section].

Sol−Gel Processing. The F-T/Q, F-T/T, and F-T/D copolymers of **1(a,b,c)(T^0)**[22] [F = (Ph)P(CH_2CH_2OMe)-(CH_2)$_x$−] and **3(a,b,c)(T^0)$_3$**[22] {F = [*cis*-Cl(H)Ru-(CO)]$_{1/3}$P(Ph)(CH_2CH_2OMe)(CH_2)$_x$−} were obtained by mixing the corresponding monomers with Si(OEt)$_4$ (**Q^0**), MeSi(OMe)$_3$ (**T^0**), or Me$_2$Si(OEt)$_2$ (**D^0**) in the presence of the catalyst and an excess of water (see Scheme 3). In the case of the F-T/Q copolymers it is necessary to add a minimum amount of alcohol to the mixture to establish homogeneous reaction conditions. The addi-

---

(12) Breitscheidel, B.; Zieder, J.; Schubert, U. *Chem. Mater.* **1991**, *3*, 559.

(13) Lindner, E.; Schreiber, R.; Kemmler, M.; Schneller, T.; Mayer, H. A. *Chem. Mater.* **1995**, *7*, 951.

(14) Lindner, E.; Schreiber, R.; Schneller, T.; Wegner, P.; Mayer, H. A.; Göpel, W.; Ziegler, Ch. *Inorg. Chem.* **1996**, *35*, 514.

(15) Fyfe, C. A. *Solid State NMR for Chemists*; CRC Press: Guelph, ON, 1984.

(16) Engelhardt, G.; Michel, D. *High Resolution Solid-State NMR of Silicates and Zeolites*; John Wiley and Sons: Chichester, 1987; p 106.

(17) Schmidt-Rohr, K.; Spiess, H. W. *Multidimensional Solid State NMR and Polymers*; Academic Press: London, 1994.

(18) Schmidt-Rohr, K.; Clauss, J.; Spiess, H. W. *Macromolecules* **1992**, *25*, 3273.

(19) Lindner, E.; Bader, A.; Glaser, E.; Pfleiderer, B.; Schumann, W.; Bayer, E. *J. Organomet. Chem.* **1988**, *355*, 45.

(20) Lindner, E.; Kemmler, M.; Mayer, H. A. *Chem. Ber.* **1992**, *125*, 2385.

(21) Lindner, E.; Schreiber, R.; Kemmler, M.; Mayer, H. A.; Fawzi, R.; Steimann, M. *Z. Anorg. Allg. Chem.* **1993**, *619*, 202.

(22) Nomenclature of the compounds. *Integer*: type of reactive center (**1** = ligand, **2** = complex); *small letter*: type of spacer (**a** = *n*-propyl, **b** = *n*-hexyl, **c** = *n*-octyl); *capital letter*: type of silicon species (**Q** = four oxygen bonds, **T** = three oxygen bonds, **D** = two oxygen bonds); *subscript*: stoichiometry of the silicon species: *superscript*: number of Si−O−Si bonds.

(23) Bader, A.; Lindner, E. *Coord. Chem. Rev.* **1991**, *108*, 27.

Scheme 2

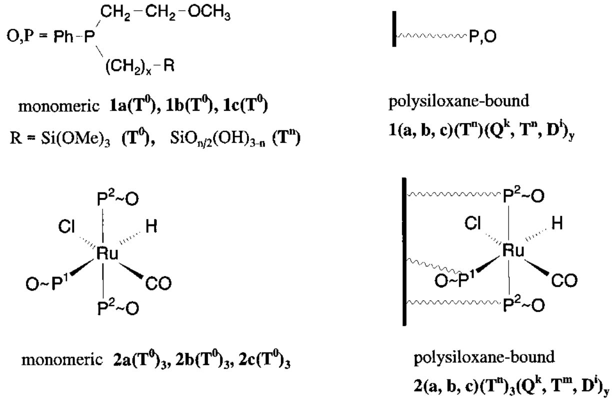

monomeric **1a(T^0), 1b(T^0), 1c(T^0)**

R = $Si(OMe)_3$ (**T^0**), $SiO_{n/2}(OH)_{3-n}$ (**T^n**)

polysiloxane-bound

1(a, b, c)(T^n)(Q^k, T^n, D^i)$_y$

monomeric **$2a(T^0)_3$, $2b(T^0)_3$, $2c(T^0)_3$**

polysiloxane-bound

2(a, b, c)$(T^n)_3$(Q^k, T^m, D^i)$_y$

x	monomers ligands	 complexes
3 (*n*-propyl)	**1a(T^0)**	**$3a(T^0)_3$**
6 (*n*-hexyl)	**1b(T^0)**	**$3b(T^0)_3$**
8 (*n*-octyl)	**1c(T^0)**	**$3c(T^0)_3$**

i, k, m, n = number of Si-O-Si bonds (k = 0-4; n, m = 0-3; i = 0-2)

y = number of cocondensated Q, T, D silicon atoms

P~O: η^1-P-coordinated ether-phosphine ligand $PhP(CH_2CH_2OMe)(CH_2)_xSi(OMe)_3$ and $PhP(CH_2CH_2OMe)(CH_2)_xSiO_{n/2}(OH)_{3-n}$, respectively

x = length of the spacer [x = 3 (**a**), 6 (**b**), 8 (**c**)]

Q^k: Q type silicon atom (four oxygen neighbors)

$T^{m,n}$: T type silicon atom (three oxygen neighbors)

D^i: D type silicon atom (two oxygen neighbors)

Scheme 3

Idealized Polycondensation

$$\underset{\substack{\mathbf{1(a,b,c)(T^0)}\\ \mathbf{2(a,b,c)(T^0)_3}}}{\text{F-Si(OMe)}_3} + \underset{\mathbf{Q^0}}{2\ \text{Si(OEt)}_4} \xrightarrow[\text{-3 MeOH, -8 EtOH}]{(3/2 + 4)\ \text{H}_2\text{O}} \underset{\substack{\mathbf{1(a,b,c)(T^3)(Q^4)_2}\\ \mathbf{2(a,b,c)(T^3)_3(Q^4)_6}}}{[\text{F-SiO}_{3/2}][\text{SiO}_{4/2}]_2} \tag{1}$$

Realistic Composition of the Polycondensate: $[\text{F-SiO}_{n/2}(\text{OX})_{3-n}][\text{SiO}_{k/2}(\text{OX})_{4-k}]_y$

1(a, b, c)(T^n)$(Q^k)_y$, 2(a, b, c)$(T^n)_3(Q^k)_y$

Idealized Polycondensation

$$\underset{\substack{\mathbf{1(a,b,c)(T^0)}\\ \mathbf{2(a,b,c)(T^0)_3}}}{\text{F-Si(OMe)}_3} + \underset{\mathbf{T^0}}{2\ \text{MeSi(OMe)}_3} \xrightarrow[\text{-9 MeOH}]{9/2\ \text{H}_2\text{O}} \underset{\substack{\mathbf{1(a,b,c)(T^3)(T^3)_2}\\ \mathbf{2(a,b,c)(T^3)_3(T^3)_6}}}{[\text{F-SiO}_{3/2}][\text{MeSiO}_{3/2}]_2} \tag{2}$$

Realistic Composition of the Polycondensate: $[\text{F-SiO}_{n/2}(\text{OX})_{3-n}][\text{MeSiO}_{m/2}(\text{OX})_{3-m}]_y$

1(a, b, c)(T^n)$(T^m)_y$, 2(a, b, c)$(T^n)_3(T^m)_y$

Idealized Polycondensation

$$\underset{\substack{\mathbf{1(a,b,c)(T^0)}\\ \mathbf{2(a,b,c)(T^0)_3}}}{\text{F-Si(OMe)}_3} + \underset{\mathbf{D^0}}{2\ \text{Me}_2\text{Si(OEt)}_2} \xrightarrow[\text{- 3 MeOH, - 4 EtOH}]{(3/2 + 2)\ \text{H}_2\text{O}} \underset{\substack{\mathbf{1(a,b,c)(T^3)(D^2)_2}\\ \mathbf{2(a,b,c)(T^3)_3(D^2)_6}}}{[\text{F-SiO}_{3/2}][\text{Me}_2\text{SiO}_{2/2}]_2} \tag{3}$$

Realistic Composition of the Polycondensate: $[\text{F-SiO}_{n/2}(\text{OX})_{3-n}][\text{Me}_2\text{SiO}_{i/2}(\text{OX})_{2-i}]_y$

1(a, b, c)(T^n)$(D^i)_y$, 2(a, b, c)$(T^n)_3(D^i)_y$

F = $(Ph)P(CH_2CH_2OMe)(CH_2)_x$- (**1a, 1b, 1c**)

F = $[HRuCl(CO)]_{1/3}P(Ph)(CH_2CH_2OMe)(CH_2)_x$- (**2a, 2b, 2c**)

Q^k: Q type silicon atom (four oxygen neighbors)

$T^{n,m}$: T type silicon atom (three oxygen neighbors)

D^i: D type silicon atom (two oxygen neighbors)

k, i, m, n = number of Si-O-Si bonds

X = H, Me, Et

y = real number of cocondensed Q, T, D silicon atoms

x = length of the spacer [x = 3 (**a**), 6 (**b**), 8(**c**)]

Table 1. Labeling of the Copolymers[22]

monomeric ligands	spacer length[a]	co-condensate **Q^0** $[Si(OEt)_4]$	 **T^0** $[MeSi(OMe)_3]$	 **D^0** $[Me_2Si(OEt)_2]$
		(a) Co-Condensed Ligands		
1a(T^0)	3	**1a(T^n)$(Q^k)_2$**[b]	**1a(T^n)$(T^m)_2$**[c]	**1a(T^n)$(D^i)_{1.5}$**[c]
1b(T^0)	6	**1b(T^n)$(Q^k)_2$**	**1b(T^n)$(T^m)_2$**	**1b(T^n)$(D^i)_{1.1}$**
1c(T^0)	8	**1c(T^n)$(Q^k)_2$**	**1c(T^n)$(T^m)_2$**	**1c(T^n)$(D^i)_{1.4}$**

monomeric complexes	spacer length[a]	co-condensate **Q^0** $[Si(OEt)_4]$	 **T^0** $[MeSi(OMe)_3]$	 **D^0** $[Me_2Si(OEt)_2]$
		(b) Co-Condensed Complexes		
$2a(T^0)_3$	3	**$2a(T^n)_3(Q^k)_6$**[b]	**$2a(T^n)_3(T^m)_6$**[c]	**$2a(T^n)_3(D^i)_{4.6}$**[c]
$2b(T^0)_3$	6	**$2b(T^n)_3(Q^k)_6$**	**$2b(T^n)_3(T^m)_6$**	**$2b(T^n)_3(D^i)_{3.3}$**
$2c(T^0)_3$	8	**$2c(T^n)_3(Q^k)_6$**	**$2c(T^n)_3(T^m)_6$**	**$2c(T^n)_3(D^i)_{1.5}$**

[a] Number of methylene groups between phosphorus and silicon in ligand **1**. [b] See also ref 6. [c] See also ref 13.

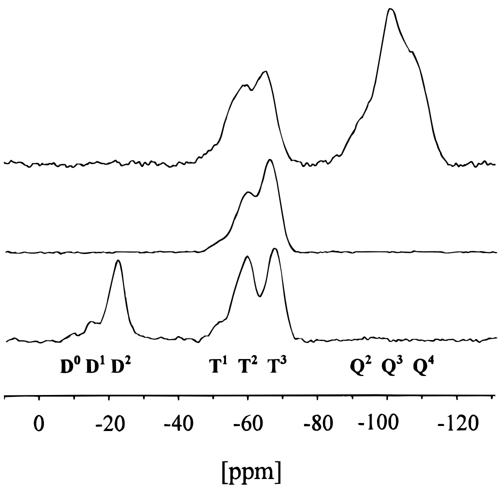

Figure 1. ^{29}Si CP MAS NMR spectra of the polymers **$2c(T^n)_3(Q^k)_6$** (top), **$2c(T^n)_3(T^m)_6$** (middle), and **$2c(T^n)_3(D^i)_{1.5}$** (bottom) including the chemical shift ranges of the different silyl species.

tion of supplementary alcohol is not necessary in the case of F-T/T and F-T/D copolymers since the alcohol which is formed during the hydrolysis reaction homogenizes the reaction mixture within minutes. To maintain uniform reaction conditions for all polycondensation reactions mentioned in this paper, only $Sn(OAc)_2(n\text{-}Bu)_2$ was used as the polycondensation catalyst. The applied stoichiometries were chosen to be 1:2 between the functionalized F−**T^0** groups and the co-condensates **Q^0**, **T^0**, and **D^0**, respectively. Since the total condensation of all Si−OH groups is normally not achieved, e.g. **D^0**, **D^1**, **T^1**, **T^2**, **Q^2**, and **Q^3** silyl species are present in the ^{29}Si solid-state NMR spectra (vide infra), an excess amount of water has to be involved in the sol−gel reaction to obtain a high degree of hydrolysis. All polycondensation products are summarized in Table 1.

^{29}Si Solid-State NMR Spectroscopic Characterization of the Matrixes. If the mobilities of the matrixes should be related to their spacer length, it has to be ensured that the corresponding polysiloxane matrixes have comparable stoichiometries and degrees of cross-linkage.

In Figure 1 the ^{29}Si CP/MAS NMR spectra of the polymers **$2c(T^n)_3(Q^k)_6$**, **$2c(T^n)_3(T^m)_6$**, and **$2c(T^n)_3(D^i)_{1.5}$** are displayed. The typical chemical shifts of the various silyl species are also shown in this figure.[24,25] To estimate the quantitative ratios of the silyl species and therefore the degree of condensation,[26] first the peak

---

(24) Maciel, G. E.; Sindorf, D. W. *J. Am. Chem. Soc.* **1980**, *102*, 7606.

(25) Williams, E. A. NMR Spectroscopy of Organosilicon Compounds. In *Chemistry of Organic Silicon Compounds*; Patai, S., Rappoport, Z., Eds.; Wiley: New York, 1989.

Table 2. Relative I_0, T_{SiH}, and $T_{1\rho H}$ Data of the Silyl Groups of the T/Q Copolymers

compound	relative I_0 data of T and Q species						degree of condensation [%]		real T/Q moiety	T_{SiH} [ms][a]					$T_{1\rho H}$ [ms][b]
	T^1	T^2	T^3	Q^2	Q^3	Q^4	T	Q		T^2	T^3	Q^2	Q^3	Q^4	
1a(T^n)(Q^k)$_2$[c,d]		1.9	8.1	1.6	8.7	7.9	94	84	1:1.8	0.94	1.00		1.11	2.77	2.5
1b(T^n)(Q^k)$_2$[c]		2.7	7.3	2.7	4.8	10.5	91	86	1:1.8	0.57	0.83	0.62	0.92	1.36	1.6
1c(T^n)(Q^k)$_2$[c]		5.4	4.6	3.4	9.5	6.0	82	78	1:1.9	0.49	0.85	0.40	1.12	2.34	3.4
2a(T^n)$_3$(Q^k)$_6$[d,e]	0.6	3.0	6.4	2.1	9.3	8.3	86	83	3:5.9	1.27	1.53	1.27	1.51	2.54	5.5
2b(T^n)$_3$(Q^k)$_6$[e]	0.2	5.5	4.3	2.1	8.1	7.4	80	83	3:5.4	1.04	1.20	1.01	1.44	2.69	5.3
2c(T^n)$_3$(Q^k)$_6$[e]		5.2	4.8	1.8	13.1	6.0	83	80	3:6.3	1.11	1.36		1.29	3.21	5.0

[a] Determined by contact time variation. [b] Determined via ^{29}Si with experiment according to Schaefer (see Experimental Section). [c] I_0 values from deconvoluted ^{29}Si MAS NMR (SPE) spectra. [d] See also ref 6. [e] I_0 values calculated from eq 1.

Table 3. Relative I_0, T_{SiH}, $T_{1\rho H}$, and T_{1Si} Data of the Silyl Groups of the T/T Copolymers

compound	relative I_0 data[a]			degree of condensation [%]	T_{SiH} [ms][b]		$T_{1\rho H}$[c] [ms]	T_{1Si} [s][d]	
	T^1	T^2	T^3		T^2	T^3		T^2	T^3
1a(T^n)(T^m)$_2$[e]	0.3	2.2	7.5	91	0.70	1.04	2.2		
1b(T^n)(T^m)$_2$		2.2	7.8	93	1.17	1.15	2.9		
1c(T^n)(T^m)$_2$		2.0	8.0	93	0.93	1.08	2.3	45.2	52.2
2a(T^n)$_3$(T^m)$_6$[e]	1.1	3.3	5.6	82	1.32	1.92	5.2	26.5	30.2
2b(T^n)$_3$(T^m)$_6$	0.2	3.6	6.2	87	1.22	1.61	5.4	18.7	20.7
2c(T^n)$_3$(T^m)$_6$	0.4	4.2	5.4	83	1.46	1.88	5.2	17.9	20.4

[a] I_0 values calculated from eq 1. [b] Determined by contact time variation. [c] Determined via ^{29}Si with experiment according to Schaefer (see Experimental Section). [d] Values from the NMR experiment of Torchia (see Experimental Section). [e] See also ref 13.

Table 4. Relative I_0, T_{SiH}, and $T_{1\rho H}$ Data of the Silyl Groups of the T/D Copolymers

compound	relative I_0 data of T and D species[a]						degree of condensation [%]		real T/D moiety	T_{SiH} [ms][b]				$T_{1\rho H}$ [ms][c]
	T^1	T^2	T^3	D^0	D^1	D^2	T	D		T^2	T^3	D^1	D^2	
1a(T^n)(D^i)$_{1.5}$[d]		2.8	7.2	0.3	0.7	13.9	91	96	1:1.5	*e*	*e*	*e*	*e*	3.6
1b(T^n)(D^i)$_{1.1}$		2.7	7.3		0.5	10.0	91	98	1:1.1	1.54	1.55	2.27	2.28	4.3
1c(T^n)$_3$(D^i)$_{1.4}$			10.0			14.0	100	100	1:1.4		1.40		2.40	5.1
2a(T^n)$_3$(D^i)$_{4.6}$[d]	0.3	4.6	5.1	0.6	2.5	12.3	83	88	3:4.6	0.99	1.26		2.12	6.0
2b(T^n)$_3$(D^i)$_{3.3}$	0.5	3.8	5.7	0.3	3.9	6.7	84	82	3:3.3	1.40	1.48	1.23	1.43	5.1
2c(T^n)$_3$(D^i)$_{1.5}$	0.8	4.8	4.4	0.2	1.8	3.1	78	80	3:1.5	1.55	1.81	0.98	1.47	5.1

[a] Calculated from eq 1. [b] Determined by contact time variation. [c] Determined via ^{29}Si with experiment according to Schaefer (see Experimental Section). [d] See also ref 13. [e] $T_{SiH} \approx T_{1\rho H}$; a precise determination of T_{SiH} is therefore impossible.

areas of the silicon atoms have to be determined by peak deconvolution of the ^{29}Si CP/MAS NMR spectra. Second the obtained peak areas of the silyl species have to be corrected due to the different cross polarization and relaxation parameters T_{SiH} and $T_{1\rho H}$. Subsequently a quantitative determination of the relative amount I_0 of the silyl species in the T/Q, T/T, and T/D blends can be drawn by the application of eq 1, using the boundary condition $T_{SiH} \ll T_{1\rho H}$:[27]

$$I_{(Tc)} = \frac{I_0}{1 - T_{SiH}/T_{1\rho H}}(e^{-T_c/T_{1\rho H}} - e^{-T_c/T_{SiH}}) \qquad (1)$$

The essential T_{SiH} data were obtained by contact time studies of each sample and the $T_{1\rho H}$ values by the pulse sequence according to Schaefer[28] (Tables 2–4).

The functionalized T/Q copolymers show degrees of condensation from 80 to 94% for the T^n groups and 78 to 86% for the Q^k groups (Table 2). The T:Q ratios are in acceptable agreement with the applied stoichiometries of 1:2 and 3:6, respectively. The T_{SiH} values are dominated by the number of OH groups per silicon atom. Therefore the fully condensed Q^4 groups with rather long ^{29}Si–H distances magnetize slowest. Since the decays of magnetization in the $T_{1\rho H}$ experiment are monoexponential in each of the samples the material can be considered as homogeneous and the formation of domains of "bulk silica" can be excluded.[6,29,30] It is therefore possible to detect even the Q^4 units quantitatively by using the cross-polarization method. The relative amounts of I_0 of the different silyl species of the polycondensed ligands **1(a,b,c)(T^n)(Q^k)$_2$** were obtained by direct deconvolution of the ^{29}Si single-pulse-excitation (SPE) MAS NMR spectra of these compounds, since the boundary condition of $T_{SiH} \ll T_{1\rho H}$ is not fulfilled in these cases.

The ^{29}Si CP/MAS NMR spectroscopic data of the T/T blends indicate that the matrixes are not affected by the type of spacer used (Table 3). Uniform degrees of condensation of 91–93% for the immobilized ligands **1(a,b,c)(T^n)(T^m)$_2$** and 82–87% for the immobilized complexes **2(a,b,c)(T^n)$_3$(T^m)$_6$**, as well as similar relaxation times are in agreement with earlier investigations.[13]

The experimentally detected stoichiometries of the functionalized T/D copolymers differ significantly from the applied stoichiometries (Table 4). Some of the D groups are washed out during the sol–gel process.[13] But

---

(26) The degree of condensation of the T species: $100(T^1 + 2T^2 + 3T^3)/[3(T^1 + T^2 + T^3)]$, degree of condensation of the Q species: $100(2Q^2 + 3Q^3 + 4Q^4)/[4(Q^2 + Q^3 + Q^4)]$, degree of condensation of the D species: $100(D^1 + 2D^2)/[2(D^1 + D^2)]$.

(27) Harris, R. K. *Analyst* **1985**, *110*, 649.

(28) Schaefer, J.; Stejskal, E. O.; Buchdahl, R. *Macromolecules* **1977**, *10*, 384.

(29) Koenig, J. L.; Andreis, M. *Solid State NMR of Polymers*; Mathias, L. J., Ed.; Plenum Press: New York, 1991; p 201.

(30) Komoroski, R. A. *High Resolution NMR Spectroscopy of Synthetic Polymers in Bulk*; VCH Publishers, Inc.: Deerfield Beach, FL, 1986; p 63.

at least the degrees of condensation as well as the ^{29}Si NMR spectroscopic relaxation data are comparable within the limits of error.

As a result of the ^{29}Si CP/MAS NMR spectroscopic investigations, it can be concluded that the different lengths of the spacers e.g. the different ligands **1(a−c)(T^0)** and complexes **2(a−c)(T^0)$_3$**, do not influence the structure of the resulting polysiloxane matrixes. The matrixes of the corresponding co-condensates show comparable degrees of condensation with the exception of **1c(T^n)(Q^k)$_2$**.[31]

^{31}P, ^{13}C CP/MAS, and IR Spectroscopic Characterization of the Polymers. In the ^{31}P CP/MAS NMR spectra of the polysiloxane-bound ether−phosphines **1-(a,b,c)(T^n)(Q^k,T^m,D^i)$_y$** only one signal is observed (see Figure 2 and Table 5). Their chemical shifts in the range −30.7 to −31.7 ppm are comparable to those observed by ^{31}P{^{1}H} NMR spectroscopy in solution (see Experimental Section and ref 19). No other phosphine species or phosphine oxides are detectable in the spectra of the freshly prepared polymers, but heating of the materials in the presence of air for several hours leads to a decomposition and the formation of phosphorus containing species which resonate at −22.6 and 34.1 ppm.[10,32] The ^{31}P CP/MAS NMR spectra of the immobilized ruthenium(II) complexes **2(a,b,c)(T^n)$_3$-(Q^k,T^m,D^i)$_y$** are displayed in Figure 3. They show two isotropic signals caused by the different environments of the phosphorus nuclei P^2 and P^1 (Scheme 2). Their chemical shifts are in agreement with their monomeric congeners (see Table 5 and Experimental Section). The occurrence of only one absorption band in the carbonyl region of the IR spectra also confirms that the structure of the complex *cis*-H(Cl)Ru(CO)(P∼O)$_3$ is preserved during the sol−gel process.

The resonances in the ^{13}C CP/MAS NMR spectra of the polymers consist mainly of four groups of peaks belonging to the following species. The phenyl groups in the aromatic region from 138.8 to 128.4 ppm, the carbon atoms in the ligands adjacent to the ether oxygen atoms [OCH$_3$ (58.0−58.8 ppm) and CH$_2$O (68.2−70.1 ppm)], a complex pattern of methylene groups in the region between 32 and 10 ppm and in case of the F-T/T and F-T/D blends one signal of the SiCH$_3$ groups at −1 to −3 ppm. These chemical shifts clearly indicate the integrity of the phosphine ligands, in particular the existence of intact carbon−phosphorus and carbon−silicon bonds.[33]

Mobility Studies of the Polymeric Ligands and Complexes by ^{31}P CP/MAS NMR and 2D WISE NMR Spectroscopy. Interphases are designed to be able to imitate homogeneous reaction types. Therefore detailed knowledge of the dynamic behavior of the stationary phases is necessary to optimize the reactivity of the catalytic centers. Higher mobilities of the immobilized catalysts should enhance the accessibility and the uniformity of the reactive centers and thus their activities as well as their selectivities. The NMR parameters T_{PH}, T_{1P}, $T_{1\rho H}$, and the line widths of the ^{31}P signals in the CP/MAS NMR spectra and of the protons in the two-dimensional WISE spectra are sensitive toward motions on different time scales.

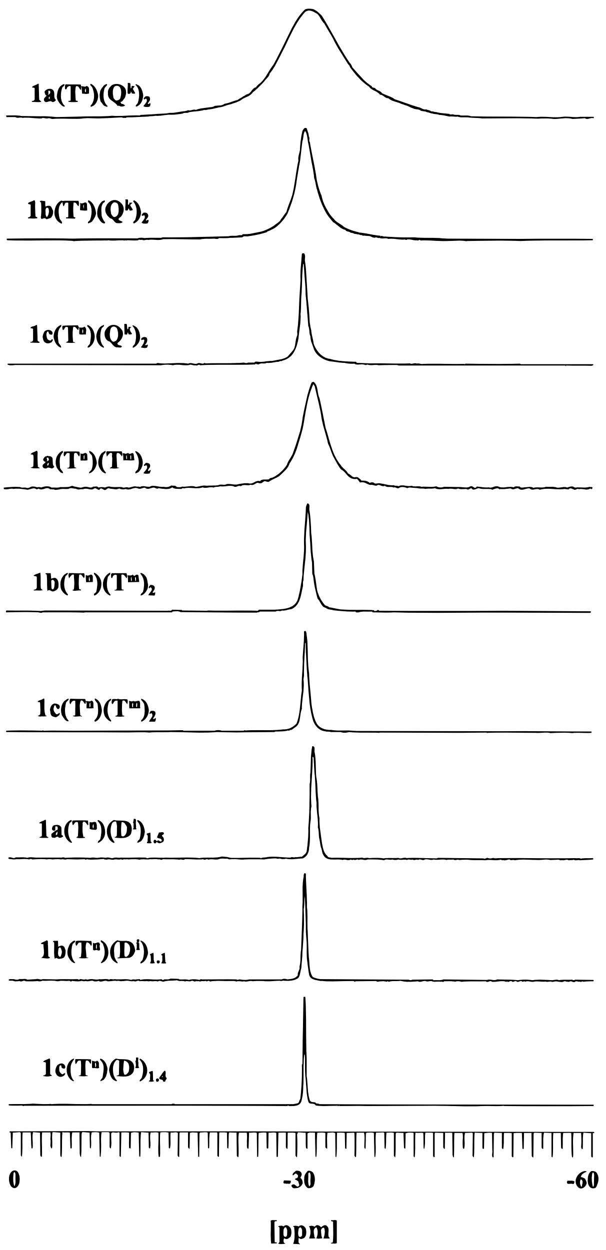

Figure 2. ^{31}P CP MAS NMR spectra of the polysiloxane-bound ether−phosphine ligands (ν_{rf} = 5 kHz).

The line widths of ^{31}P solid-state NMR spectra are governed by various interactions, e.g., chemical shift dispersion, chemical shift anisotropy (CSA), and heteronuclear dipolar interactions.[15] Since the local environment of the phosphorus atoms in the ligands and complexes of the different copolymers are identical, the changes of the line widths of the ^{31}P signals in the CP/MAS NMR spectra are caused by the variable flexibilities of the materials. The cross-polarization constants T_{PH} depend on the distance and number of surrounding protons and on the rigidity of the corresponding internuclear vector, e.g., between phosphorus and protons. However, if the phosphorus atoms of various compounds are surrounded by equal or very similar numbers of protons, the cross-polarization constants are solely determined by their mobilities. Fast motions in the kilohertz region led to inefficient cross-polarization and

---

(31) The lower degree of condensation of copolymer **1c(T^n)(Q^k)$_2$** compared to the corresponding F-T/Q polysiloxane-bound ligands **1-(a,b)(T^n)(Q^k)$_2$** cannot be explained yet, since the kinetic rates of the various hydrolysis and condensation steps are not known.

(32) Blümel, J. *GIT Fachz. Lab.* **1994**, *5*, 510.

(33) Corriu, R. J. P.; Moreau, J. J. E.; Thepot, P.; Wong Chi Man, M. *J. Mater. Chem.* **1994**, *4*, 987.

Table 5. ^{31}P CP/MAS, T_{PH}, $T_{1\rho H}$, T_{1P}, and T_g Data of the Polysiloxane-Bound Ether−Phosphine Ligands 1 and Complexes 2

(a) Ligands

compound	δ ^{31}P [ppm]	T_{PH} [ms][a]	$T_{1\rho H}$ [ms][b]	$\nu_{1/2}$ [Hz]	T_{1P} [s][c]	T_g [°C]
$1a(T^n)(Q^k)_2$	−31.7	0.29	1.36	900	7.0	d
$1b(T^n)(Q^k)_2$	−31.0	0.32	1.38	270	4.4	d
$1c(T^n)(Q^k)_2$	−30.8	0.52	1.39	89	2.7	d
$1a(T^n)(T^m)_2$	−31.6	0.36	1.57	340	6.9	−5.8
$1b(T^n)(T^m)_2$	−31.0	0.56	1.05	96	2.6	−31.9
$1c(T^n)(T^m)_2$	−30.7	0.71	2.01	71	2.4	−35.9
$1a(T^n)(D^i)_{1.5}$	−31.7	2.01	6.90	90	1.9	−53.6
$1b(T^n)(D^i)_{1.1}$	−30.8	1.79	3.58	46	2.0	−61.2
$1c(T^n)(D^i)_{1.4}$	−30.8	2.15	7.18	20	1.3	−60.7

(b) Complexes

compound	δ ^{31}P [ppm]	T_{PH} [ms][a]	$T_{1\rho H}$ [ms][b]	$\nu_{1/2}$ [Hz]	T_{1P} [s][c]
$2a(T^n)_3(Q^k)_6$	17.1	0.22	2.6	2800	8.7
	−0.9	0.23	2.6		8.4
$2b(T^n)_3(Q^k)_6$	17.5	0.19	4.8	2030	11.3
	−0.8	0.21	4.8		11.2
$2c(T^n)_3(Q^k)_6$	17.7	0.19	4.8	1740	11.0
	−0.9	0.21	5.0		11.1
$2a(T^n)_3(T^m)_6$	17.6	0.19	2.9	2600	6.2
	0.5	0.21	2.6		6.0
$2b(T^n)_3(T^m)_6$	18.0	0.21	5.5	1780	12.3
	−0.7	0.20	5.6		12.4
$2c(T^n)_3(T^m)_6$	18.0	0.19	4.1	1580	12.8
	−1.2	0.21	4.0		12.7
$2a(T^n)_3(D^i)_{4.6}$	17.5	0.20	3.8	2060	7.0
	−0.7	0.23	3.8		7.1
$2b(T^n)_3(D^i)_{3.3}$	18.1	0.19	4.3	1645	13.0
	0.1	0.21	4.3		12.8
$2c(T^n)_3(D^i)_{1.5}$	17.7	0.19	4.6	1560	13.1
	−1.7	0.27	4.4		14.1

[a] Determined by contact time variation. [b] Determined via ^{31}P with the experiment according to Schaefer (see Experimental Section). [c] Values from the NMR experiment of Torchia (see Experimental Section) at 297 K. [d] No glass transitions were detected in the temperature range between −110 and 140 °C.

therefore higher T_{PH} values.[34−37] The relaxation time of the protons in the rotating frame $T_{1\rho H}$ is an averaged quantity within domains of 1−2 nm in diameter in those cases where sufficient dipolar coupling among the protons provides spin diffusion.[28,29] In cases with enhanced mobilities in the kilohertz region dipolar coupling among protons becomes inefficient and specific $T_{1\rho H}$ values for certain parts of the material can be obtained. The spin−lattice relaxation times T_{1P} are characteristic values for each nucleus and sensitive toward motions in the megahertz region.[15,38] However unambiguous information about mobilities of molecules or molecule fragments from T_{1P} or $T_{1\rho H}$ data can be obtained only if the corresponding correlation times τ_R are known. The relation between the correlation time τ_R and the relaxation times T_{1P} and $T_{1\rho H}$ is given by the correlation−time curve.[15] Temperature-dependent relaxation time measurements can distinguish between two cases. In the slow-motion regime, decreasing relaxation times correlate with decreasing τ_R (increasing temperature) and thus faster motions, whereas in the fast-motion regime the relaxation times are increasing with faster motions (shorter τ_R).

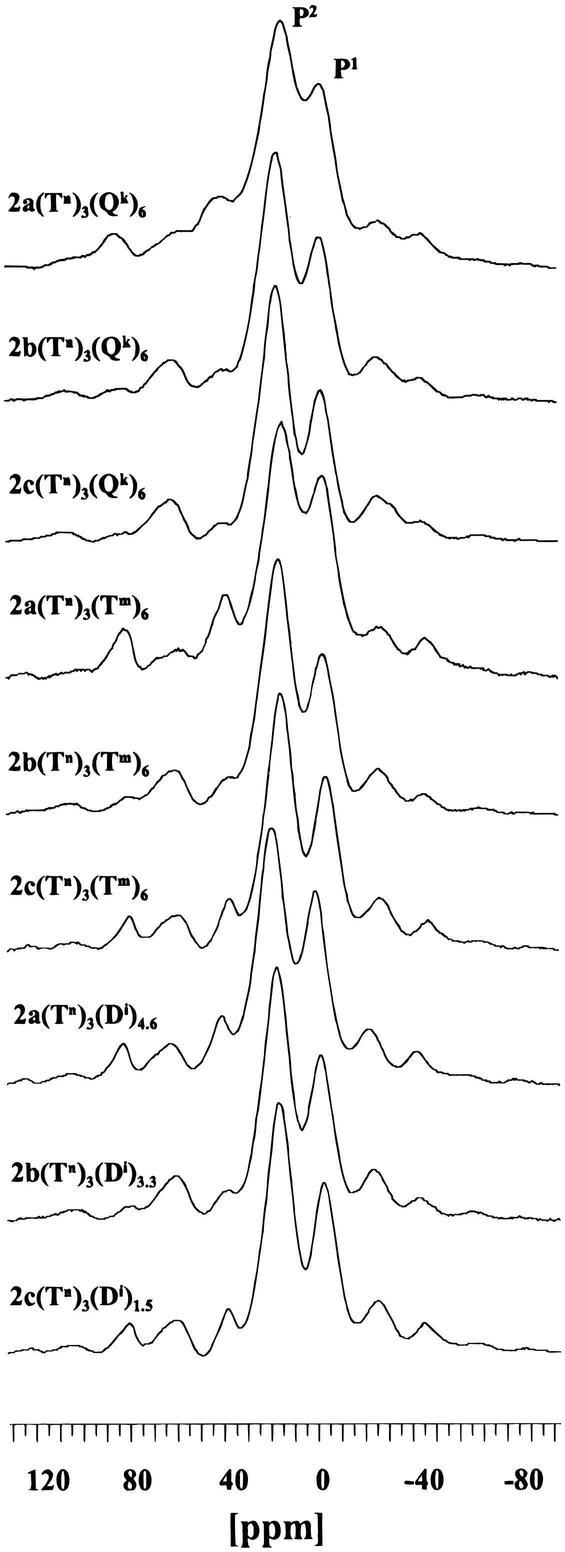

Figure 3. ^{31}P CP MAS NMR spectra of the polysiloxane-bound ruthenium(II) complexes (ν_{rf} = 5 kHz).

The pulse sequence of the WISE experiment consists of a ^1H $\pi/2$ pulse followed by an incremented proton evolution time (t_1), after which the proton magnetization is transferred to ^{13}C via Hartmann−Hahn cross polarization, i.e., $\pi/2(^1H)-t_1-CP-$acquisition.[18] Slices at individual ^{13}C resonances in a 2D data set reveal the ^1H line widths of the various structural moieties within a sample. The line widths in the F1 (proton) dimension

---

(34) Schmid-Betschinger, J. Ph.D. Dissertation, Universität Tübingen, 1989.

(35) Veemann, W. S.; Menger, E. M.; Ritchey, W.; de Boer, E. *Macromolecules* **1979**, *12*, 924.

(36) Sullivan, M. J.; Maciel, G. E. *Anal. Chem.* **1982**, *54*, 1606.

(37) Earl, W. L.; VanderHart, D. L. *Macromolecules* **1979**, *12*, 762.

(38) Voelkel, R. *Angew. Chem., Int. Ed. Engl.* **1988**, *27*, 1468.

are determined by ^{1}H$-^{1}$H dipolar interactions, which are reduced by molecular motion and magic angle spinning.

The line widths of the ^{31}P CP/MAS NMR signals of the polysiloxane-bound ligands are listed in Table 5, and the corresponding spectra are displayed in Figure 2. It is obvious that the line widths in all cases decrease in the series F-T/Q > F-T/T ≫ F-T/D for each spacer length. Also the line widths decrease if the spacer becomes longer. Simultaneously the T_{PH} values increase for a given spacer from 0.29 ms for **1a(T^{n})(Q^{k})$_{2}$** to 2.01 ms for **1a(T^{n})(D^{i})$_{1.5}$**. The cross-polarization constants T_{PH} of the F-T/T and F-T/Q copolymers containing a longer spacer are larger than for the shorter *n*-propyl spacer, e.g., 0.29 ms for **1a(T^{n})(Q^{k})$_{2}$**, 0.32 for **1b(T^{n})(Q^{k})$_{2}$**, and 0.52 for **1c(T^{n})(Q^{k})$_{2}$**. The decrease of the line widths from 900 Hz [**1a(T^{n})(Q^{k})$_{2}$**] to 20 Hz [**1c(T^{n})(D^{i})**$_{1.4}$] accompanied by a slower magnetization transfer, e.g., longer T_{PH} values, leads to the conclusion that the mobilities of the various polymer-bound ligands are affected by the type of the cocondensate in the order F-T/Q < F-T/T ≪ F-T/D.[34−37] This is in agreement with earlier results, which demonstrated, that a decrease of the absolute crosslinkage leads to an increase of the mobility of the phosphorus atoms.[6,13] In addition the line widths and cross-polarization constants T_{PH} also depend on the spacer length. The extension of the spacer from *n*-propyl via *n*-hexyl to *n*-octyl raises the mobilities of the phosphorus atoms. These results are confirmed by the spin−lattice relaxation times T_{1P} of the polymers. From temperature-dependent studies it is known that the T_{1P} values of the copolymers **1a(T^{n})(Q^{k})$_{2}$**[6] and **1c(T^{n})(Q^{k})$_{2}$** [T_{1P} (297 K) 2.7 s; T_{1P} (315 K) 2.3 s; T_{1P} (325 K) 2.2 s] decrease with increasing temperature. Thus shorter T_{1P} times correspond to shorter correlation times τ_R and thus to higher mobilities in the megahertz region.[15] The T_{1P} value at room temperature of the highly mobile material **1c(T^{n})(D^{i})$_{1.4}$** is already in the extremely narrowing-limit since T_{1P} increases from 1.3 s (297 K) to 1.7 s (307 K) and 1.8 s (317 K). The extraordinary mobility of the F-T/D copolymers is also established by their high $T_{1\rho H}$ values, indicating higher mobilities because the relaxation times $T_{1\rho H}$ of the polymers are located in the fast-motion regime of the correlation time curve [$T_{1\rho H}$ of **1c(T^{n})(Q^{k})$_{2}$** 1.39 ms (297 K), 1.88 ms (305 K), 2.60 ms (315 K), 3.10 ms (315 K); $T_{1\rho H}$ of **1c(T^{n})(D^{i})$_{1.4}$** 7.18 ms (297 K), 8.64 ms (305 K), 16.10 ms (315 K)]. Large $T_{1\rho H}$ values thus are identical with an inefficient dipolar-relaxation mechanism caused by fast motion in the kilohertz region.

To get a more detailed knowledge about the mobilities of different parts of the polymer, the two-dimensional wideline-separation (WISE) NMR spectroscopy was applied. In Figure 4 the WISE spectra of the polymer **1c(T^{n})(D^{i})$_{1.4}$** is depicted. The narrow lines of about 5 kHz in the F1 dimension indicating high mobilities in the region of some 10 kHz confirm the results of the ^{31}P relaxation data. The polysiloxane-bound ligand **1c(T^{n})(D^{i})$_{1.4}$** behaves like a polymer above glass transition temperature T_g.[17] The WISE spectra of the more rigid copolymer **1c(T^{n})(T^{m})$_{2}$** display much broader line widths of the resonances at 30 and 0 ppm (Figure 5), demonstrating that the polysiloxane backbone of the F-T/T polymer is much more rigid than the corresponding backbone of the F-T/D blend. The resonances of the aromatic region and the ether moiety of compound **1c(T^{n})(T^{m})$_{2}$** are narrower than those of the methylene groups of the alkyl chain, being consistent with an increase of the mobility along the spacer.

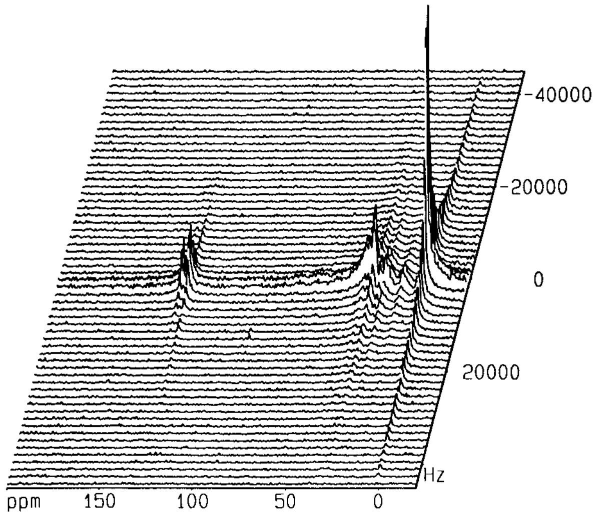

Figure 4. WISE spectrum of polymer-bound ligand **1c(T^{n})(D^{i})$_{1.4}$**.

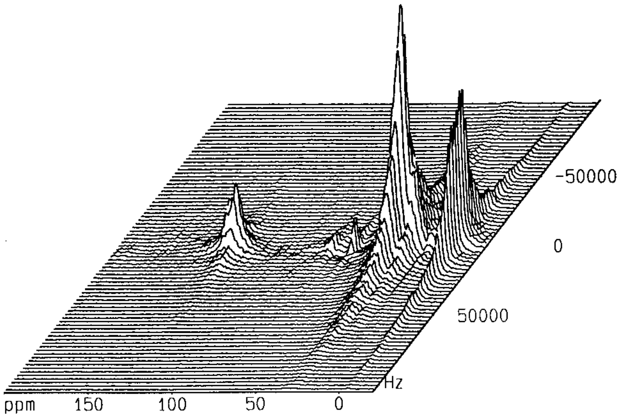

Figure 5. WISE spectrum of polymer-bound ligand **1c(T^{n})(T^{m})$_{3}$**.

The NMR data are confirmed by differential scanning calorimetric (DSC) measurements (see Table 5). The glass transition temperatures T_g for the F-T/T and F-T/D copolymers are observed in the range between −5.8 °C [**1a(T^{n})(T^{m})$_{2}$**] and −61.2 °C [**1b(T^{n})(D^{i})$_{1.1}$**] (Table 5). In the case of the F-T/Q bound ligands no glass transition could be detected. The T_g values of the F-T/D bound ligands are lower than those of the corresponding F-T/T blends, indicating again the higher mobility of the less cross-linked F-T/D copolymers. The extension of the spacer length from 3 to 6 or 8 also leads to a decrease of the T_g values, being consistent with a restricted flexibility of the shorter *n*-propyl spacers.

We were also interested if the different mobilities of the noncomplexed ether−phosphines ligands **1(a,b,c)(T^{n})(Q^{k},T^{m},D^{i})$_{y}$** lead to different mobilities of the corresponding P-coordinated ether−phosphine ruthenium(II) complexes. Again the line widths in the ^{31}P CP/MAS NMR spectra of the immobilized complexes **2(a,b,c)(T^{n})$_{3}$(Q^{k},T^{m},D^{i})$_{y}$** decrease in the order of the spacers *n*-propyl ≫ *n*-hexyl > *n*-octyl and also in the order of the copolymers F-T/Q > F-T/T ≫ F-T/D (see Table 5 and Figure 3). But the differences of the line widths are not as significant as in the spectra of the

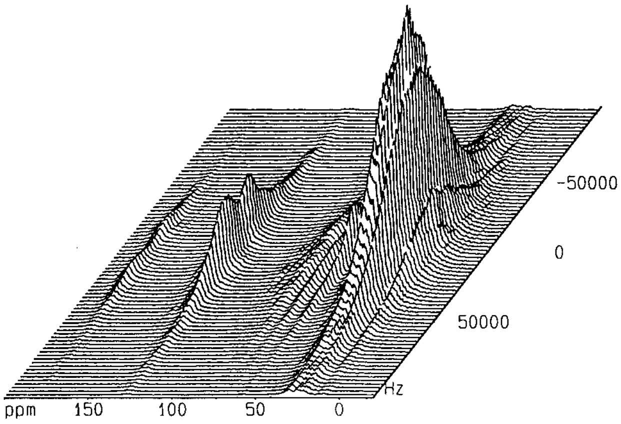

Figure 6. WISE spectrum of polymer-bound complex **$2c(T^n)_3(Q^k)_6$**.

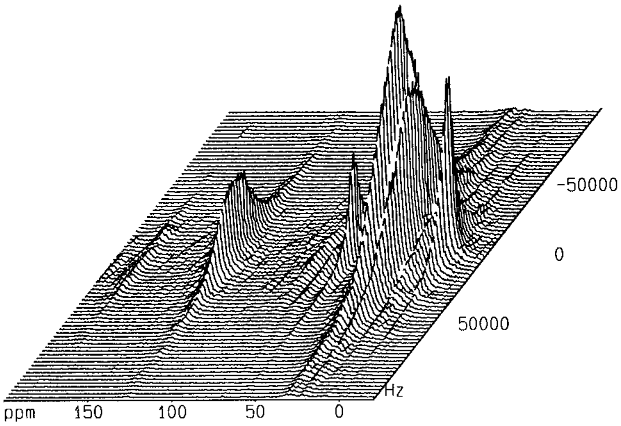

Figure 7. WISE spectrum of polymer-bound complex **$2c(T^n)_3(D^i)_{1.5}$**.

corresponding ligands. The T_{PH} values drop to 0.2 ms for all polymers (Table 5). Obviously the P-coordination of the ligands enables a fast magnetization transfer for all types of co-condensates and spacers. The $T_{1\rho H}$ relaxation times of the polysiloxane-bound complexes are first decreasing and then increasing on going from room temperature to higher temperatures,[6] indicating a strong dipolar interaction of the protons at room temperature. Thus conclusions about segmental mobilities cannot be drawn from this parameter.[39,40] Compared to the ligands the long T_{1P} values of the polysiloxane-bound complexes (7−14 s) again emphasize the reduced mobility due to the phosphorus−metal coordination.

The 2D WISE spectra of the polymers **$2c(T^n)_3(Q^k)_6$** (Figure 6) and **$2c(T^n)_3(D^i)_{1.5}$** (Figure 7) confirm the findings that the polysiloxane-bound complexes are more rigid than the corresponding polysiloxane-bound ligands. The line widths of the methylene groups (25−31 ppm) are about 50 kHz, which is approximately twice the value of compound **$1c(T^n)(T^m)_2$** (Figure 5). The Gaussian line shapes of the methylene resonances (Figures 6 and 7) compared to the triangle type line shape of the methylene groups of the polysiloxane-bound ligand **$1c(T^n)(T^m)_2$** (Figure 5) indicate the higher mobilities of the noncomplexed ligands, too.[17] The line widths in the proton dimension of the resonances of the polymer **$2c(T^n)_3(Q^k)_6$** (Figure 6) are approximately 10 kHz broader than in the case of the polymer **$2c(T^n)_3(D^i)_{1.5}$** confirming the results of ^{31}P CP/MAS NMR line-widths analysis. In both WISE spectra the smallest line widths in the F1 dimension are observed for the methyl groups [OCH_3 (near 58 ppm) and $SiCH_3$ (near 0 ppm)] due to their fast rotation.

Conclusion

Remarkable differences in the mobilities of polysiloxane-bound ether−phosphine ligands were detected. The extension of the spacer length from *n*-propyl via *n*-hexyl to *n*-octyl as well as the use of the less cross-linking co-condensates T and D enhance the flexibility of the matrixes. The coordination of three ether−phosphine ligands to one ruthenium center leads to an additional cross-linking of the matrixes and therefore strongly reduces the mobility of the coordinating phosphorus atoms. The differences in the mobilities detected on "free" ligands related to the type of co-condensate and spacer almost vanish. From the line widths of the ^{31}P CP/MAS NMR spectra, it is concluded that the mobilities of the phosphorus atoms can be ranked in the same way as for the polysiloxane-bound ether−phosphines. But the interpretation of other ^{31}P solid-state NMR relaxation data is not as unambiguous as in the case of the polymer-anchored ligands. The 2D WISE NMR experiment has shown too that the differences of the mobilities of the immobilized ruthenium(II) complexes are quite small. The results of the ^{31}P solid-state NMR line widths studies could be established exemplarily. In contrast to the polysiloxane-bound ligands where an enhancement of the mobilities along the alkyl chain was detected by 2D WISE spectroscopy, the analogous polysiloxane-bound complexes do not show this phenomena. This is due to the additional cross-linkage of the ligands at the ruthenium center. However, we expect that larger differences in the mobilities will occur with complexes which are anchored to only one or two ligands.

Experimental Section

The elemental analyses were carried out on a Carlo Erba Model 1106 analyzer. IR data were obtained on a Bruker IFS 48 FT-IR spectrometer. The solution nuclear magnetic resonance spectra (NMR) were recorded on a Bruker AC 80 [^{31}P{^{1}H}] and a Bruker AC 250 [^{13}C{^{1}H} and ^{1}H] spectrometer. The frequencies, standards, and temperatures are as follows: ^{31}P{^{1}H} NMR: 32.44 MHz, external 85% H_3PO_4 in acetone-d_6, 243 K. ^{13}C{^{1}H} NMR: 62.90 MHz, internal standard TMS, 300 K. ^{1}H NMR: 250.13 MHz, internal standard TMS, 300 K. Mass spectra (field desorption) were acquired on a Finnigan MAT 711A modified by AMD Mess- and Datensysteme (8 kV, 60 °C) and are reported as mass/charge (*m*/*z*). The differential scanning calorimetric (DSC) measurements were recorded on a Mettler DSC 820 equipment on 10 mg gels. The heating rate was 20 K/min. The data were analyzed by the Mettler Toledo software TA 8000. The glass transition temperature was determined as the midpoint in the DSC curve.

The CP/MAS solid-state NMR spectra were recorded on a Bruker MSL 200 (4.7 T) multinuclear spectrometer (^{29}Si) and a Bruker ASX 300 (7.05 T) spectrometer (^{13}C and ^{31}P) equipped with wide-bore magnets. Magic angle spinning was applied at 3 kHz (^{29}Si), 5 kHz (^{31}P), and 10−12 kHz (^{13}C). All measurements were carried out under exclusion of molecular oxygen. Frequencies and standards: ^{31}P, 121.49 MHz [85% H_3PO_4, $NH_4H_2PO_4$ (δ = 0.8) as the second standard]; ^{13}C, 50.325 MHz [TMS, carbonyl resonance of glycin (δ = 170.09) as the second standard]; ^{29}Si, 39.75 MHz (Q_8M_8). The cross-

---

[39] Douglas, D. C.; McBrierty, V. J. *J. Chem. Phys.* **1971**, *54*, 4085.
[40] Assink, R. A.; Wilkes, G. C. *J. Polym. Eng. Sci.* **1977**, *17*, 606.

polarization constants T_{PH} and T_{SiH} were determined by variations of the contact time (20−25 experiments). The proton relaxation time in the rotating frame $T_{1\rho H}$ was measured by direct proton spin lock−τ−CP experiments as described by Schaefer and Stejskal.[28] T_{1P} and T_{1Si} values were received using the method developed by Torchia.[41] The relaxation time data were obtained by using the Bruker software SIMFIT or Jandel software PEAKFIT. Three times the highest T_{SiH} value has been used as a typical contact time T_C for the quantitative determination of the relative amount of the silyl species with eq 1. Peak deconvolution of the spectra were performed with the Bruker-Spectrospin software XNMR using Voigtian line shapes. The WISE NMR spectra were recorded under MAS conditions (4 kHz). Between 40 and 64 t_1 increments with a dwell time of 3−10 μs were used for each spectrum. Cross polarization was applied with contact times between 200 and 400 μs. For a more detailed description of other NMR parameters see ref 6.

All manipulations were performed under argon by employing the usual Schlenk techniques. Methanol was dried with magnesium and distilled; ethanol was distilled from NaOEt. *n*-Hexane and toluene were distilled from sodium benzophenone ketyl. H_2O, $Si(OEt)_4$ (**Q⁰**, Aldrich), $MeSi(OMe)_3$ (**T⁰**, Aldrich), and $Me_2Si(OEt)_2$ (**D⁰**, Aldrich) were distilled under inert gas prior to use. All solvents were stored under argon. The ether−phosphines **1(a,b)(T⁰)**,[19] the starting complexes *cis*-$Cl(H)Ru(CO)(PPh_3)_3$,[42] and **2a(T⁰)₃**[6] were synthesized as described previously.

(2-Methoxyethyl)(phenyl)(8-(trimethoxysilyl)octyl)-phosphine [1c(T⁰)]. The synthesis of **1c(T⁰)** was carried out in accordance with the literature[19] by a photochemical addition of $HP(Ph)CH_2CH_2OCH_3$ (8.41 g, 50 mmol) and 8-(trimethoxysilyl)oct-1-ene (12.78 g, 55 mmol) to give a colorless liquid [yield of **1c(T⁰)**: 13.63 g, 68%]. $^{31}P\{^1H\}$ NMR (toluene) δ −33.9; $^{13}C\{^1H\}$ NMR ($CDCl_3$) δ 9.1 (s, CH_2Si), 22.5 (s, CH_2-CH_2Si), 25.9 [d, $^1J_{PC}$ = 14.1 Hz, $PCH_2(CH_2)_7$], 28.2 [s, $CH_2(CH_2)_2$-Si], 28.6 [d, $^2J_{PC}$ = 24.1 Hz, $PCH_2CH_2(CH_2)_6$], 29.0 [2s, $P(CH_2)_3CH_2CH_2$], 31.1 [d, $^1J_{PC}$ = 11.7 Hz, $PCH_2CH_2OCH_3$], 33.0 [s, $PCH_2CH_2CH_2$], 50.3 (s, $SiOCH_3$), 58.3 (s, CH_2OCH_3), 70.1 [d, $^2J_{PC}$ = 20.6 Hz, $PCH_2CH_2OCH_3$], 128.3 [d, $^3J_{PC}$ = 6.9 Hz, *m*-C_{arom}], 128.7 (s-, *p*-C_{arom}), 132.3 [d, $^2J_{PC}$ = 19.1 Hz, *o*-C_{arom}], 138.5 [d, $^1J_{PC}$ = 14.8 Hz, *i*-C_{arom}]; FD-MS *m/z* 400.5 (M^+, 100). Anal. Calcd for $C_{20}H_{37}O_4PSi$: C, 59.97; H, 9.31. Found: C, 60.07; H, 8.97.

Preparation of the T⁰-Functionalized Ether−Phosphine Ruthenium Complexes 2b(T⁰)₃ and 2c(T⁰)₃. *cis*-$Cl(H)Ru(CO)(PPh_3)_3$ was refluxed for 1 h with 3 equiv of **1(b,c)T⁰** in toluene. After evaporation of the solvent under vacuum, the slightly yellow oils were dissolved in *n*-hexane (200 mL) at 60 °C, and the solutions were allowed to stand 12 h at −50 °C to separate the products. This procedure was repeated to remove PPh_3.

Carbonylchlorohydridotris[(2-methoxyethyl)phenyl-(6-(trimethoxysilyl)hexyl)phosphine-*P,P′,P″*]ruthenium-(II)(Tᵐ)₆ [2b(T⁰)₃]. A suspension of **1b(T⁰)** (330 mg, 0.886 mmol) and *cis*-$Cl(H)Ru(CO)(PPh_3)_3$ (281 mg, 295 mmol) in toluene (20 mL) was refluxed for 30 min and treated with *n*-hexane to form a slightly yellow oil [yield of **2b(T⁰)₃**: 208 mg, 55%]. ^1H NMR (C_6D_6) δ −7.14 [dt, $^2J_{PH}$ = 110, $^2J_{PH}$ = 26 Hz, RuH]; $^{31}P\{^1H\}$ NMR (toluene) δ 17.8−13.9 (m, P^2), −2.4 to −4.6 (m, P^1); $^{13}C\{^1H\}$ NMR (C_6D_6) δ 13.6 (CH_2Si), 23.0−26.5 ($PCH_2(CH_2)_3CH_2CH_2Si$), 29.2−32.9 [$PCH_2(CH_2)_3$, PCH_2-CH_2OCH_3], 50.3 ($SiOCH_3$), 58.3 (CH_2OCH_3), 68.8−69.4 ($PCH_2CH_2OCH_3$), 127.6−134.3 (*i*-, *o*-, *m*-, *p*-C_{arom}), 203.5 [q, $^2J_{PC}$ = 13.9 Hz, RuCO]; IR (film on NaCl, cm^{-1}) 1911 [ν(CO)]; FD-MS *m/z* 1283 (M^+, 10), 910 [M^+ − **1b(T⁰)**, 45], 874 [M^+ − **1b-(T⁰)** − Cl, 55], 372 [**1b(T⁰)**, 100]. Anal. Calcd for $C_{55}H_{100}ClO_{13}P_3RuSi_3$: C, 51.49; H, 7.86; Cl, 2.76; Ru, 7.88. Found: C, 51.88; H, 8.51; Cl, 2.41; Ru, 7.54.

Carbonylchlorohydridotris[(2-methoxyethyl)phenyl-(6-(trimethoxysilyl)octyl)phosphine-*P,P′,P″*]ruthenium-(II)(Tᵐ)₆ [2c(T⁰)₃]. A suspension of **1c(T⁰)** (202 mg, 0.630 mmol) and *cis*-$Cl(H)Ru(CO)(PPh_3)_3$ (200 mg, 210 mmol) in toluene (20 mL) was refluxed for 30 min and treated with *n*-hexane to form a slightly yellow oil [yield of **2c(T⁰)₃**: 143.6 mg, 50%]. ^1H NMR (C_6D_6) δ −7.13 [dt, $^2J_{PH}$ = 110, $^2J_{PH}$ = 26 Hz, RuH]; $^{31}P\{^1H\}$ NMR (toluene) δ 17.8−14.0 (m, P^2), −2.1 to −3.4 (m, P^1); $^{13}C\{^1H\}$ NMR (C_6D_6) δ 9.1 (CH_2Si), 22.5 (CH_2-CH_2Si), 25.9−32.3 [$P(CH_2)_6$], 50.3 ($SiOCH_3$), 58.3 (CH_2OCH_3), 70.1 ($PCH_2CH_2OCH_3$), 127.5−139.3 (*i*-, *o*-, *m*-, *p*-C_{arom}), 203.7 [q, $^2J_{PC}$ = 14 Hz, RuCO]; IR (film on NaCl, cm^{-1}) 1911 [ν(CO)]; FD-MS *m/z* 965.3 [M^+ − **1c(T⁰)**, 20], 930.4 [M^+ − **1c(T⁰)** − Cl, 11], 401 [**1c(T⁰)**, 100]. Anal. Calcd for $C_{61}H_{112}ClO_{13}P_3RuSi_3$: C, 53.59; H, 8.13; Cl, 2.59; Ru, 7.05. Found: C, 53.89; H, 8.48; Cl, 2.20; Ru, 7.39.

Sol−Gel Processing. The polysiloxane-bound ligands **1-(b,c)(Tⁿ)(Qᵏ)₂**, **1(b,c)(Tⁿ)(Tᵐ)₂**, and **1(b,c)(Tⁿ)₃(Dⁱ)*ᵧ*** (y = 1.1 or 1.4) and complexes **2(b,c)(Tⁿ)₃(Qᵏ)₆**, **2(b,c)(Tⁿ)₃(Tᵐ)₆**, and **2(b,c)(Tⁿ)₃(Dⁱ)*ᵧ*** (y = 3.3 or 1.5) were sol−gel processed in an analogous way as already described for **1a(Tⁿ)(Qᵏ,Tᵐ,Dⁱ)*ᵧ*** (y = 2, 2, or 1.5) and **2a(Tⁿ)₃(Qᵏ,Tᵐ,Dⁱ)*ᵧ*** (y = 6, 6, or 4.5).[6,13] The solid-state NMR spectroscopic data of these polymers are published elsewhere in detail.[6,13] Here the ^{31}P CP/MAS NMR spectra and relaxation times have been recorded at 121.49 MHz for reasons of comparability.

(2-Methoxyethyl)phenyl(polysiloxanylhexyl)phosphine-(Qᵏ)₂ [1b(Tⁿ)(Qᵏ)₂]. A mixture of the O,P ligand **1b(T⁰)** (1.0 g, 2.684 mmol), 2 equiv of $Si(OEt)_4$ (**Q⁰**) (1.113 g, 5.368 mmol), water (531 mg, 29.524 mmol), and $(n\text{-}Bu)_2Sn(OAc)_2$ (13 mg, 0.038 mmol) was sol−gel processed to give a colorless gel. After solvent processing and aging a white powder was formed [yield of **1b(Tⁿ)(Qᵏ)₂**: 1.046 g, 92%]: ^{13}C CP/MAS NMR δ 9.7 (CH_2-Si), 22.8 (CH_2CH_2Si), 26.7 [$PCH_2(CH_2)_3$] 28.8−32.6 [$PCH_2(CH_2)_3$, $PCH_2CH_2OCH_3$], 58.0 (CH_2OCH_3), 69.9 ($PCH_2CH_2OCH_3$), 128.8 (*m*-, *p*-C_{arom}), 132.3 (*o*-C_{arom}), 138.8 (*i*-C_{arom}); ^{29}Si MAS NMR (SPE, silicon substructure) δ −57.7 (T^2), −65.1 (T^3), −91.9 (Q^2), −100.2 (Q^3), −107.3 (Q^4). Anal. Calcd for $C_{15}H_{24}O_{6.5}PSi_3$[43] (idealized stoichiometry): C, 42.53; H, 5.71. Corrected stoichiometry:[44] C, 39.31; H, 5.89. Found: C, 39.62; H, 5.71.

(2-Methoxyethyl)phenyl(polysiloxanyloctyl)phosphine-(Qᵏ)₂ [1c(Tⁿ)(Qᵏ)₂]. A mixture of the O,P ligand **1c(T⁰)** (670 mg, 1.673 mmol), 2 equiv of $Si(OEt)_4$ (**Q⁰**) (679 mg, 3.346 mmol), water (331 mg, 18.403 mmol), and $(n\text{-}Bu)_2Sn(OAc)_2$ (13 mg, 0.038 mmol) was sol−gel processed to give a colorless gel. After solvent processing and aging a white powder was formed [yield of **1c(Tⁿ)(Qᵏ)₂**: 749 mg, 99%]: ^{13}C CP/MAS NMR δ 14.1 (CH_2Si), 18.2 ($SiOCH_2CH_3$), 22.9 (CH_2CH_2Si), 26.7 [PCH_2-$(CH_2)_3$] 28.8−32.6 [$PCH_2(CH_2)_5$, $PCH_2CH_2OCH_3$], 50.7 ($SiOCH_3$), 58.1 (CH_2OCH_3), 66.2 ($SiOCH_2CH_3$), 70.3 ($PCH_2CH_2OCH_3$), 128.8 (*m*-, *p*-C_{arom}), 132.2 (*o*-C_{arom}), 138.8 (*i*-C_{arom}); ^{29}Si MAS NMR (SPE, silicon substructure) δ −57.0 (T^2), −64.5 (T^3), −90.2 (Q^2), −100.5 (Q^3), −107.0 (Q^4). Anal. Calcd for $C_{17}H_{28}O_{6.5}$-PSi_3[43] (idealized stoichiometry): C, 45.17; H, 6.25. Corrected stoichiometry:[44] C, 41.41; H, 6.66. Found: C, 42.31; H, 6.84.

(2-Methoxyethyl)phenyl(polysiloxanylhexyl)phosphine-(Tᵐ)₂ [1b(Tⁿ)(Tᵐ)₂]. A mixture of the O,P ligand **1b(T⁰)** (1.0 g, 2.684 mmol), 2 equiv of $MeSi(OMe)_3$ (**T⁰**) (729 mg, 5.368 mmol), water (280 mg, 14.470 mmol), and $(n\text{-}Bu)_2Sn(OAc)_2$ (13 mg, 0.038 mmol) was sol−gel processed to give a colorless gel. After solvent processing and aging a white powder was formed [yield of **1b(Tⁿ)(Tᵐ)₂**: 1.207 g, 103%]: ^{13}C CP/MAS NMR δ −3.1 ($SiCH_3$), 13.8 (CH_2Si), 22.9 (CH_2CH_2Si), 25.6 [PCH_2-$(CH_2)_3$] 28.3−31.0 [$PCH_2(CH_2)_3$, $PCH_2CH_2OCH_3$], 49.7 ($SiOCH_3$), 58.0 (CH_2OCH_3), 70.1 ($PCH_2CH_2OCH_3$), 128.4 (*m*-, *p*-C_{arom}), 132.2 (*o*-C_{arom}), 138.2 (*i*-C_{arom}); ^{29}Si CP/MAS NMR (silicon substructure) δ −57.9 (T^2), −65.7 (T^3). Anal. Calcd for $C_{17}H_{30}O_{5.5}PSi_3$[43] (idealized stoichiometry): C, 46.65; H, 6.91. Corrected stoichiometry:[44] C, 45.50; H, 7.03. Found: C, 45.41; H, 6.58.

(2-Methoxyethyl)phenyl(polysiloxanyloctyl)phosphine-(Tᵐ)₂ [1c(Tⁿ)(Tᵐ)₂]. A mixture of the O,P ligand **1c(T⁰)** (670

---

[41] Torchia, A. D. *J. Magn. Reson.* **1978**, *30*, 613.

[42] Ahmad, N.; Levison, J. J.; Robinson, S. D.; Uttley, M. F. *Inorg. Synth.* **1974**, *15*, 48.

[43] The broken numbers in the chemical formulas are due to $SiO_{3/2}$ units or to the amount of Q, T, or D silicon units.

[44] The corrected stoichiometry was obtained by adding the additional number of OH units of the Q^2, Q^3, T^1, T^2, and D^1 groups (obtained from the ^{29}Si CP/MAS NMR spectra) to the idealized stoichiometry (only Q^4, T^3, and D^2 units).

mg, 1.673 mmol), 2 equiv of MeSi(OMe)$_3$ (**T^0**) (456 mg, 3.346 mmol), water (271 mg, 15.057 mmol), and (*n*-Bu)$_2$Sn(OAc)$_2$ (13 mg, 0.038 mmol) was sol−gel processed to give a colorless gel. After solvent processing and aging a white powder was formed [yield of **1c(T^n)(T^m)$_2$**: 805 mg, 103%]: ^{13}C CP/MAS NMR δ −2.9 (SiCH$_3$), 13.8 (CH$_2$Si), 23.1 (*C*H$_2$CH$_2$Si), 25.7 [P*C*H$_2$(CH$_2$)$_3$] 28.2−31.2 [PCH$_2$(*C*H$_2$)$_5$, P*C*H$_2$CH$_2$OCH$_3$], 58.0 (CH$_2$O*C*H$_3$), 70.2 (PCH$_2$*C*H$_2$OCH$_3$), 128.5 (*m*-, *p*-C$_{arom}$), 132.2 (*o*-C$_{arom}$), 138.1 (*i*-C$_{arom}$); ^{29}Si CP/MAS NMR (silicon substructure) δ −58.5 (T^2), −65.8 (T^3). Anal. Calcd for $C_{19}H_{34}O_{5.5}PSi_3$[43] (idealized stoichiometry): C, 49.00; H, 7.36. Corrected stoichiometry:[44] C, 47.86; H, 7.47. Found: C, 48.03; H, 7.32.

(2-Methoxyethyl)phenyl(polysiloxanylhexyl)phosphine-(D^i)$_{1.1}$ [1b(T^n)(D^i)$_{1.1}$]. A mixture of the O,P ligand **1b(T^0)** (1.0 g, 2.684 mmol), 2 equiv of Me$_2$Si(OEt)$_2$ (**D^0**) (796 mg, 5.368 mmol), water (202 mg, 11.300 mmol), and (*n*-Bu)$_2$Sn(OAc)$_2$ (32 mg, 0.090 mmol) was sol−gel processed to give a colorless rubber. After solvent processing and aging a white powder was formed [yield of **1b(T^n)(D^i)$_{1.1}$**: 0.913 g, 75%]: ^{13}C CP/MAS NMR δ 1.1 (SiCH$_3$), 13.9 (CH$_2$Si), 23.2 (*C*H$_2$CH$_2$Si), 26.0 [P*C*H$_2$(CH$_2$)$_3$] 28.7 [PCH$_2$*C*H$_2$CH$_2$*C*H$_2$, P*C*H$_2$CH$_2$OCH$_3$], 33.1 [P(CH$_2$)$_2$*C*H$_2$], 58.4 (CH$_2$O*C*H$_3$), 70.1 (PCH$_2$*C*H$_2$OCH$_3$), 128.5 (*m*-, *p*-C$_{arom}$), 132.4 (*o*-C$_{arom}$), 138.1 (*i*-C$_{arom}$); ^{29}Si CP/MAS NMR (silicon substructure) δ −13.3 (D^1), −21.7 (D^2), −58.7 (T^2), −67.5 (T^3). Anal. Calcd for $C_{17.2}H_{30.6}O_{3.6}PSi_{2.1}$[43] (idealized stoichiometry): C, 53.66; H, 7.77. Corrected stoichiometry:[44] C, 51.84; H, 7.90. Found: C, 48.40; H, 7.48.

(2-Methoxyethyl)phenyl(polysiloxanyloctyl)phosphine-(D^i)$_{1.4}$ [1c(T^n)(D^i)$_{1.4}$]. A mixture of the O,P ligand **1c(T^0)** (670 mg, 1.673 mmol), 2 equiv of Me$_2$Si(OEt)$_2$ (**D^0**) (496 mg, 3.346 mmol), water (211 mg, 11.711 mmol), and (*n*-Bu)$_2$Sn(OAc)$_2$ (32 mg, 0.090 mmol) was sol−gel processed to give a colorless rubber. After solvent processing and aging a white powder was formed [yield of **1c(T^n)(D^i)$_{1.4}$**: 0.740 g, 92%]: ^{13}C CP/MAS NMR δ 1.3 (SiCH$_3$), 14.2 (CH$_2$Si), 23.4 (*C*H$_2$CH$_2$Si), 26.2 [P*C*H$_2$(CH$_2$)$_3$] 29.5 [P*C*H$_2$CH$_2$OCH$_3$, PCH$_2$*C*H$_2$, P(CH$_2$)$_5$*C*H$_2$], 31.5 [P(CH$_2$)$_2$*C*H$_2$*C*H$_2$], 58.0 (CH$_2$O*C*H$_3$), 70.1 (PCH$_2$*C*H$_2$OCH$_3$), 128.5 (*m*-, *p*-C$_{arom}$), 132.4 (*o*-C$_{arom}$), 138.1 (*i*-C$_{arom}$); ^{29}Si CP/MAS NMR (silicon substructure) δ −21.7 (D^2), −68.0 (T^3). Anal. Calcd for $C_{19.8}H_{36.4}O_{3.9}PSi_{2.4}$[43] (idealized stoichiometry): C, 54.63; H, 8.42. Corrected stoichiometry:[44] C, 54.63; H, 8.42. Found: C, 53.97; H, 8.81.

Carbonylchlorohydridotris[(2-methoxyethyl)phenyl(polysiloxanylhexyl)phosphine-*P*,*P*′,*P*″]ruthenium(II)-(Q^k)$_6$ [2b(T^n)$_3$(Q^k)$_6$]. A mixture of HRuCl(CO)(P∼O)$_3$ [**2b(T^0)$_3$**] (1.334 g, 1.040 mmol), 6 equiv of Si(OEt)$_4$ (**Q^0**) (1.297 g, 6.240 mmol), water (618 mg, 34.120 mmol), and (*n*-Bu)$_2$Sn(OAc)$_2$ (28 mg, 0.081 mmol) was sol−gel processed to give a slightly yellow gel [yield of **2b(T^n)$_3$(Q^k)$_6$**: 1.479 g, 99%]: ^{13}C CP/MAS NMR δ 13.1 (CH$_2$Si), 23.4 (*C*H$_2$CH$_2$Si), 25.6 [P*C*H$_2$(CH$_2$)$_3$], 29.8 [PCH$_2$(*C*H$_2$)$_3$, P*C*H$_2$CH$_2$OCH$_3$], 50.8 (SiOCH$_3$), 58.1 (CH$_2$O*C*H$_3$), 68.2 (PCH$_2$*C*H$_2$OCH$_3$), 128.7 (*i*-, *m*-, *o*-, *p*-C$_{arom}$); ^{29}Si CP/MAS NMR (silicon substructure) δ −49.0 (T^1), −57.1 (T^2), −64.4 (T^3), −92.9 (Q^2), −100.6 (Q^3), −107.5 (Q^4); IR (KBr, cm^{-1}) 1916 [ν(CO)]. Anal. Calcd for $C_{46}H_{73}ClO_{20.5}P_3RuSi_9$[43] (idealized stoichiometry): C, 38.47; H, 5.12; Cl, 2.47; Ru, 7.08. Corrected stoichiometry:[44] C, 35.83; H, 5.53; Cl, 2.30; Ru, 6.59. Found: C, 34.92; H, 5.46; Cl, 2.35; Ru, 7.11.

Carbonylchlorohydridotris[(2-methoxyethyl)phenyl(polysiloxanyloctyl)phosphine-*P*,*P*′,*P*″]ruthenium(II)-(Q^k)$_6$ [2c(T^n)$_3$(Q^k)$_6$]. A mixture of HRuCl(CO)(P∼O)$_3$ [**2c(T^0)$_3$**] (623 mg, 0.456 mmol), 6 equiv of Si(OEt)$_4$ (**Q^0**) (0.569 g, 2.736 mmol), water (270 mg, 14.907 mmol), and (*n*-Bu)$_2$Sn(OAc)$_2$ (28 mg, 0.081 mmol) was sol−gel processed to give a slightly yellow gel [yield of **2c(T^n)$_3$(Q^k)$_6$**: 0.670 mg, 97%]: ^{13}C CP/MAS NMR δ 13.6 (CH$_2$Si), 23.4 (*C*H$_2$CH$_2$Si), 26.5 [P*C*H$_2$(CH$_2$)$_3$] 29.7 [PCH$_2$(*C*H$_2$)$_5$, P*C*H$_2$CH$_2$OCH$_3$], 58.2 (CH$_2$O*C*H$_3$), 68.3 (PCH$_2$*C*H$_2$OCH$_3$), 128.6 (*i*-, *m*-, *o*-, *p*-C$_{arom}$); ^{29}Si CP/MAS NMR (silicon substructure) δ −57.0 (T^2), −64.9 (T^3), −91.2 (Q^2), −99.4 (Q^3), −106.6 (Q^4); IR (KBr, cm^{-1}) 1916 [ν(CO)]. Anal. Calcd for $C_{52}H_{85}ClO_{20.5}P_3RuSi_9$[43] (idealized stoichiometry): C, 41.05; H, 5.63; Cl, 2.33; Ru, 6.64. Corrected stoichiometry:[44] C, 38.21; H, 6.01; Cl, 2.17; Ru, 6.18. Found: C, 37.94; H, 6.47; Cl, 2.40; Ru, 6.91.

Carbonylchlorohydridotris[(2-methoxyethyl)phenyl(polysiloxanylhexyl)phosphine-*P*,*P*′,*P*″]ruthenium(II)-(T^m)$_6$ [2b(T^n)$_3$(T^m)$_6$]. A mixture of HRuCl(CO)(P∼O)$_3$ [**2b(T^0)$_3$**] (1.219 g, 0.950 mmol), 6 equiv of MeSi(OMe)$_3$ (**T^0**) (775 mg, 5.700 mmol), water (614 mg, 34.120 mmol), and (*n*-Bu)$_2$Sn(OAc)$_2$ (13 mg, 0.038 mmol) was sol−gel processed to give a slightly yellow gel [yield of **2b(T^n)$_3$(T^m)$_6$**: 1.327 g, 94%]: ^{13}C CP/MAS NMR δ −3.4 (SiCH$_3$), 13.3 (CH$_2$Si), 23.4 [*C*H$_2$CH$_2$Si, P*C*H$_2$(CH$_2$)$_3$] 31.1 [PCH$_2$(*C*H$_2$)$_3$, P*C*H$_2$CH$_2$OCH$_3$], 49.8 (SiOCH$_3$), 57.8 (CH$_2$O*C*H$_3$), 68.5 (PCH$_2$*C*H$_2$OCH$_3$), 128.6 (*i*-, *m*-, *o*-, *p*-C$_{arom}$); ^{29}Si CP/MAS NMR (silicon substructure) δ −50.9 (T^1), −57.0 (T^2), −65.1 (T^3); IR (KBr, cm^{-1}) 1914 [ν(CO)]. Anal. Calcd for $C_{52}H_{91}ClO_{17.5}P_3RuSi_9$[43] (idealized stoichiometry): C, 42.24; H, 6.20; Cl, 2.49; Ru, 6.84. Corrected stoichiometry:[44] C, 40.51; H, 6.41; Cl, 2.30; Ru, 6.56. Found: C, 38.41; H, 6.14; Cl, 2.52; Ru, 6.39.

Carbonylchlorohydridotris[(2-methoxyethyl)phenyl(polysiloxanyloctyl)phosphine-*P*,*P*′,*P*″]ruthenium(II)-(T^m)$_6$ [2c(T^n)$_3$(T^m)$_6$]. A mixture of HRuCl(CO)(P∼O)$_3$ [**2c(T^0)$_3$**] (745 mg, 0.545 mmol), 6 equiv of MeSi(OMe)$_3$ (**T^0**) (445 mg, 3.269 mmol), water (221 mg, 12.301 mmol), and (*n*-Bu)$_2$Sn(OAc)$_2$ (13 mg, 0.038 mmol) was sol−gel processed to give a slightly yellow gel [yield of **2c(T^n)$_3$(T^m)$_6$**: 826 mg, 97%]: ^{13}C CP/MAS NMR δ −3.3 (SiCH$_3$), 13.3 (CH$_2$Si), 23.4 (*C*H$_2$CH$_2$Si), 25.4−31.1 [P(CH$_2$)$_6$, P*C*H$_2$CH$_2$OCH$_3$], 50.1 (SiOCH$_3$), 57.9 (CH$_2$O*C*H$_3$), 69.1 (PCH$_2$*C*H$_2$OCH$_3$), 128.6 (*i*-, *m*-, *o*-, *p*-C$_{arom}$); ^{29}Si CP/MAS NMR (silicon substructure) δ −51.1 (T^1), −58.8 (T^2), −65.8 (T^3); IR (KBr, cm^{-1}) 1913 [ν(CO)]. Anal. Calcd for $C_{58}H_{103}ClO_{17.5}P_3RuSi_9$[43] (idealized stoichiometry): C, 44.58; H, 6.64; Cl, 2.27; Ru, 6.47. Corrected stoichiometry:[44] C, 42.34; H, 6.87; Cl, 2.15; Ru, 6.14. Found: C, 41.60; H, 6.71; Cl, 2.04; Ru, 5.95.

Carbonylchlorohydridotris[(2-methoxyethyl)phenyl(polysiloxanylhexyl)phosphine-*P*,*P*′,*P*″]ruthenium(II)-(D^i)$_{3.3}$ [2b(T^n)$_3$(D^i)$_{3.3}$]. A mixture of HRuCl(CO)(P∼O)$_3$ [**2b(T^0)$_3$**] (853 mg, 0.665 mmol), 6 equiv of Me$_2$Si(OEt)$_2$ (**D^0**) (591 mg, 3.978 mmol), water (150 mg, 8.37 mmol), and (*n*-Bu)$_2$Sn(OAc)$_2$ (35 mg, 0.100 mmol) was sol−gel processed to give a slightly yellow gel [yield of **2b(T^n)$_3$(D^i)$_{3.3}$**: 798.9 mg, 74%]: ^{13}C CP/MAS NMR δ 1.0 (SiCH$_3$), 13.9 (CH$_2$Si), 23.7 [*C*H$_2$CH$_2$Si, P*C*H$_2$(CH$_2$)$_3$], 31.2 [PCH$_2$(*C*H$_2$)$_3$, P*C*H$_2$CH$_2$OCH$_3$], 57.8 (CH$_2$O*C*H$_3$), 68.6 (PCH$_2$*C*H$_2$OCH$_3$), 128.7 (*i*-, *m*-, *o*-, *p*-C$_{arom}$); ^{29}Si CP/MAS NMR (silicon substructure) δ −7.7 (D^0), −16.9 (D^1), −21.4 (D^2), −50.9 (T^1), −57.0 (T^2), −65.1 (T^3); IR (KBr, cm^{-1}) 1912 [ν(CO)]. Anal. Calcd for $C_{52.6}H_{82.8}ClO_{13.1}P_3RuSi_{6.3}$[43] (idealized stoichiometry): C, 48.21; H, 6.37; Cl, 2.71; Ru, 7.71. Corrected stoichiometry:[44] C, 45.83; H, 6.49; Cl, 2.57; Ru, 7.33. Found: C, 46.79; H, 7.16; Cl, 2.02; Ru, 8.15.

Carbonylchlorohydridotris[(2-methoxyethyl)phenyl(polysiloxanyloctyl)phosphine-*P*,*P*′,*P*″]ruthenium(II)-(D^i)$_{1.5}$ [2c(T^n)$_3$(D^i)$_{1.5}$]. A mixture of HRuCl(CO)(P∼O)$_3$ [**2c(T^0)$_3$**] (754 mg, 0.545 mmol), 6 equiv of Me$_2$Si(OEt)$_2$ (**D^0**) (485 mg, 3.269 mmol), water (150 mg, 8.37 mmol), and (*n*-Bu)$_2$Sn(OAc)$_2$ (35 mg, 0.100 mmol) was sol−gel processed to give a slightly yellow gel [yield of **2c(T^n)$_3$(D^i)$_{1.5}$**: 603.1 mg, 69%]: ^{13}C CP/MAS NMR δ 1.3 (SiCH$_3$), 14.0 (CH$_2$Si), 23.7 [*C*H$_2$CH$_2$Si, P*C*H$_2$(CH$_2$)$_3$] 30.7 [PCH$_2$(*C*H$_2$)$_3$, P*C*H$_2$CH$_2$OCH$_3$], 58.4 (CH$_2$O*C*H$_3$), 68.5 (PCH$_2$*C*H$_2$OCH$_3$), 129.4 (*i*-, *m*-, *o*-, *p*-C$_{arom}$); ^{29}Si CP/MAS NMR (silicon substructure) δ −7.8 (D^0), −15.1 (D^1), −21.2 (D^2), −51.4 (T^1), −58.5 (T^2), −66.9 (T^3); IR (KBr, cm^{-1}) 1910 [ν(CO)]. Anal. Calcd for $C_{53.5}H_{89.5}ClO_{10}P_3RuSi_{4.5}$[43] (idealized stoichiometry): C, 51.46; H, 7.23; Cl, 2.84; Ru, 8.09. Corrected stoichiometry:[44] C, 49.62; H, 7.34; Cl, 2.73; Ru, 7.80. Found: C, 50.43; H, 6.99; Cl, 2.49; Ru, 8.11.

Acknowledgment. The support of this research by the Deutsche Forschungsgemeinschaft (Forschergruppe, Grant No. Li 154/41-1) Bonn/Bad Godesberg, and by the Fonds der Chemischen Industrie, Frankfurt/Main is gratefully acknowledged. We thank Prof. P. C. Schmidt and A. Fetscher, Pharmazeutisches Institut, University of Tübingen, for DSC measurements. A.J. thanks the Fonds der Chemischen Industrie for a Doktorandenstipendium.

CM9601650